nature genetics



# Spontaneous activity of opsin apoprotein is a cause of Leber congenital amaurosis

Michael L Woodruff[1,6], Zhongyan Wang[2,6], Hae Yun Chung[2], T Michael Redmond[3], Gordon L Fain[1,4,6] & Janis Lem[2,5,6]

**Mutations in *Rpe65* disrupt synthesis of the opsin chromophore ligand 11-*cis*-retinal and cause Leber congenital amaurosis (LCA), a severe, early-onset retinal dystrophy. To test whether light-independent signaling by unliganded opsin causes the degeneration, we used *Rpe65*-null mice, a model of LCA. Dark-adapted *Rpe65*$^{-/-}$mice behaved as if light adapted, exhibiting reduced circulating current, accelerated response turn-off, and diminished intracellular calcium. A genetic block of transducin signaling completely rescued degeneration irrespective of an elevated level of retinyl ester. These studies clearly show that activation of sensory transduction by unliganded opsin, and not the accumulation of retinyl esters, causes light-independent retinal degeneration in LCA. A similar mechanism may also be responsible for degeneration induced by vitamin A deprivation.**

Mutations in *RPE65* are associated with several human retinal degenerations including LCA[1–4], autosomal recessive retinitis pigmentosa[1] and rod-cone dystrophy[5]. RPE65 is essential for synthesis of the rhodopsin ligand 11-*cis*-retinal[6], and in *Rpe65*-null mutant transgenic mice (*Rpe65*$^{-/-}$), both rods and cones degenerate[6,7]. These mice have little 11-*cis*-retinal or functional visual pigment[6,8,9] but instead have opsin apoprotein (unliganded opsin)[6] and accumulate all-*trans*-retinyl esters, precursors of 11-*cis*-retinal biosynthesis, in retinal pigment epithelial cells[6,10,11].

It is not clear why defects in RPE65 produce cell death. Accumulated retinyl esters may be toxic, but the unliganded opsin may also cause degeneration. Covalent binding of opsin with 11-*cis*-retinal holds rhodopsin in an inactive state[12]. Light absorption isomerizes 11-*cis*-retinal to all-*trans*-retinal, activating the G-protein transducin and its downstream effector, cGMP phosphodiesterase.

Unliganded opsin can also stimulate transducin at a low rate in isolated, intact photoreceptors[13,14] and in dissociated, outer segment membranes[15]. Recent evidence supports the proposal[16,17] that persistent opsin or rhodopsin signaling can cause pathology. Abnormally high opsin activity decreases photoreceptor sensitivity in rhodopsin mutants associated with dominant congenital night blindness[18], but the presence of normal functional rhodopsin prevents degeneration. Prolonged illumination produces degeneration in mutant mice defective in rhodopsin turn-off, which is rescued by introduction of a null mutation in the gene encoding rod transducin α-subunit or by dark rearing[19], showing that cascade activation produces the degeneration.

We used *Rpe65*$^{-/-}$ mice to investigate whether continuous, light-independent opsin activity causes retinal degeneration. We reasoned that spontaneous opsin activity would confer light-adapted behavior on rods, that is, diminish circulating current, reduce light sensitivity, accelerate light response kinetics and reduce intracellular calcium (**Fig. 1**) and that blocking transducin-mediated signaling (but not dark-rearing) would prevent degeneration. Our studies confirmed these predictions and unambiguously identify opsin activity as a mechanism of retinal degeneration in human LCA resulting from mutations in *RPE65*. They also provide a model for understanding a mechanism of photoreceptor cell death in a subset of human retinal degenerations.

## RESULTS

### Circulating currents are smaller

Spontaneous opsin signaling in *Rpe65*$^{-/-}$ mice should close channels in darkness and produce a smaller circulating current than in dark-adapted wild-type mice (**Fig. 1b**). To test this prediction, we recorded responses from photoreceptors of wild-type and *Rpe65*$^{-/-}$ mice to flashes of progressively greater light intensity (**Fig. 2**). The baseline value represents the circulating current of the rod in darkness on the assumption that the brightest flash closes all the channels in the outer segment[20]. The circulating current in *Rpe65*$^{-/-}$ rods (**Fig. 2a**) was much smaller than in control photoreceptors[11] (**Fig. 2b**), as though dark-adapted *Rpe65*$^{-/-}$ rods were continuously illuminated.

### Light sensitivity is diminished

Exposure of normal rods to background light decreases the sensitivity of the response to superimposed flashes. Spontaneous opsin activity in *Rpe65*$^{-/-}$ rods also would be predicted to reduce sensitivity. We therefore compared sensitivities of rods from *Rpe65*$^{-/-}$ and wild-type mice

[1]Department of Physiological Science, University of California Los Angeles, Los Angeles, California 90095, USA. [2]Molecular Cardiology Research Institute, Tufts-New England Medical Center, 750 Washington St. Box 5045, Boston, Massachusetts 02111, USA. [3]Laboratory of Retinal Cell and Molecular Biology, National Eye Institute, National Institutes of Health, Bethesda, Maryland 20892, USA. [4]Department of Ophthalmology, University of California Los Angeles, Los Angeles, California 90095, USA. [5]Department of Ophthalmology, Program in Genetics, and Tufts Center for Vision Research, Tufts University School of Medicine, Boston, Massachusetts 02111, USA. [6]These authors contributed equally to this work. Correspondence should be addressed to J.L. (jlem@tufts-nemc.org).

Published online 21 September 2003; doi:10.1038/ng1246

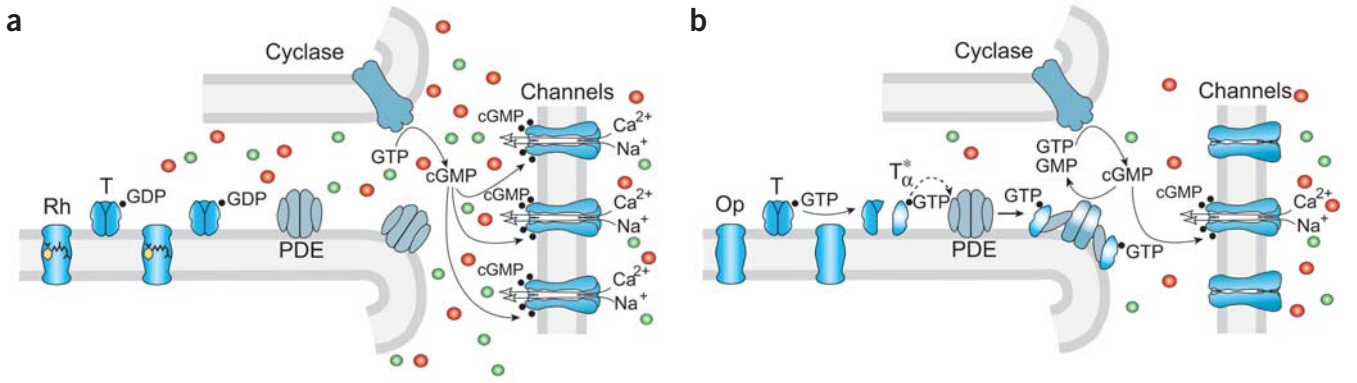


**Figure 1** Transduction and cyclic nucleotide–gated channel activity in rods. (**a**) Dark-adapted wild-type rods. In rod disk membranes, rhodopsin (Rh) liganded with 11-*cis*-retinal is prevented from activating transducin (T) and its effector, phosphodiesterase (PDE). Light-dependent isomerization of 11-*cis*-retinal to all-*trans*-retinal is required to trigger transducin and PDE activation. In the absence of light, intracellular cGMP levels remain high, holding the cGMP-gated channels in an open configuration. $Ca^{2+}$ (green dots) and $Na^+$ (red dots) pass through the channels into the cell, producing a high dark-circulating current and a high intracellular calcium concentration. (**b**) Dark-adapted *Rpe65*$^{-/-}$ rods. Opsin (Op) signals independently of light at a low rate, producing activated transducin (Tα*) that stimulates its downstream effector, PDE. Activated PDE hydrolyzes cGMP, reducing intracellular cGMP and closing a larger fraction of the cGMP-gated channels in darkness than is closed in wild-type rods. The influx of $Ca^{2+}$ and $Na^+$ into the cells is reduced. Because the $Na^+/Ca^{2+}$-$K^+$ exchanger continues to extrude $Ca^{2+}$ from the cell, the intracellular $Ca^{2+}$ concentration (green dots) is reduced, and this, together with the activation of PDE, reduces the circulating current in darkness and causes the cell to behave as if light-adapted.

by plotting the mean photocurrent response as a function of light intensity. The mean maximum response amplitude in *Rpe65*$^{-/-}$ rods was 1.4 ± 0.1 pA (mean ± s.e.m.), significantly less than the response in wild-type rods (12.2 ± 0.5 pA; $P < 0.001$; **Fig. 2c**). We expressed sensitivity as the ratio of response (in pA) to light intensity (in photons μm$^{-2}$) at intensities near threshold for the response. This sensitivity value in *Rpe65*$^{-/-}$ rods was 2.5 ± 0.2 × 10$^{-5}$ pA photon$^{-1}$ μm$^2$ (mean ± s.e.m.; $n = 58$) and in wild-type rods was 0.88 ± 0.05 pA photon$^{-1}$ μm$^2$ ($n = 39$; $P < 0.001$). The reduced sensitivity of *Rpe65*$^{-/-}$ rods partially reflects the much lower rhodopsin concentration[6–11] but is in part produced by adaptation functionally equivalent to light adaptation (see **Fig. 4**), caused by continuous opsin activation (**Fig. 1b**).

The extreme desensitization of *Rpe65*$^{-/-}$ photoreceptor cells could result from inefficient transduction with no contribution from response saturation. It was therefore important to show that the brightest flash closed all the channels in the outer segment (**Fig. 2a**). We recorded responses in the same cell to 20-ms flashes followed by a single laser flash 100 times brighter (**Fig. 3a**). The response to the laser flash was more prolonged but identical in amplitude to the saturating response produced by the brightest flash from the light bench.

## cGMP-gated channels are functional

One possible explanation for the small photocurrent amplitude of *Rpe65*$^{-/-}$ rods is that cGMP-gated channel function in outer segments was somehow compromised. We investigated channel function in two ways. First, we recorded responses of an *Rpe65*$^{-/-}$ rod to a saturating light flash and then exposed the photoreceptor to 100 μM 3-isobutyl-1-methylxanthine (IBMX), a partial competitive inhibitor that blocks photoreceptor phosphodiesterase (PDE; ref. 21), increases cGMP and increases the amplitude of the circulating current[22]. IBMX perfusion reversibly increased the amplitude of saturating responses in *Rpe65*$^{-/-}$ rods by a factor of more than 2 (**Fig. 3b**). The mean amplitude before exposure to IBMX was 1.6 ± 0.6 pA (mean ± s.e.m.; $n = 4$), increasing to 4.0 ± 0.7 pA within 120 s of IBMX addition. The mean saturating response returned to 1.3 ± 0.7 pA 3 min after we removed IBMX.

In a second approach, we looked for increased channel function after rhodopsin regeneration in *Rpe65*$^{-/-}$ rods by perfusion with 11-*cis*-retinal, as measured by changes in sensitivity and response amplitude (data not shown). *Rpe65*$^{-/-}$ rods exposed to 11-*cis*-retinal had a significantly larger circulating current (mean ± s.e.m. 5.2 ± 0.2 pA; $n = 21$) and sensitivity (0.20 ± 0.01 pA photon$^{-1}$ μm$^2$; $n = 13$) than

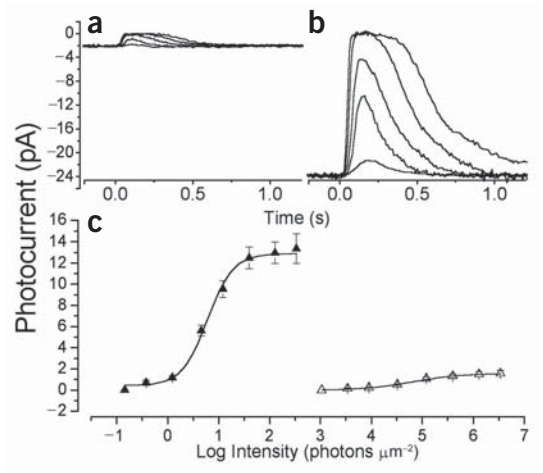


**Figure 2** Photoresponse amplitude and light sensitivity of *Rpe65*$^{-/-}$ rods are reduced. (**a**) Photoresponses of *Rpe65*$^{-/-}$ rods to 20-ms flashes of light at five intensities from near threshold to saturation. The light intensities used were 3.2 × 10$^4$, 1.2 × 10$^5$, 3.0 × 10$^5$, 1.3 × 10$^6$ and 3.4 × 10$^6$ photons μm$^{-2}$. The responses shown were averages of three rods at these stimulus intensities, and the current traces for the individual rods were obtained by averaging 5–60 flash responses. The mean saturating response for *Rpe65*$^{-/-}$ rods was 1.4 ± 0.1 pA (mean ± s.e.m.; $n = 58$ rods). (**b**) Photoresponses of control mouse (C57BL/6 strain) rods at 1.1, 4.6, 1.2 × 10$^1$, 1.3 × 10$^2$ and 3.4 × 10$^2$ photons μm$^{-2}$ . The traces shown are the average of four rods at these stimulus intensities. The mean saturating responses for control rods was 12.2 ± 0.5 pA ($n = 32$ rods). (**c**) Response-intensity data for control (filled triangles) and *Rpe65*$^{-/-}$ (open triangles) rods. The mean half-saturation was at 6.4 ± 0.5 photons μm$^{-2}$ for control rods ($n = 32$) and 4.0 × 10$^4$ photons μm$^{-2}$ for *Rpe65*$^{-/-}$ rods ($n = 16$).

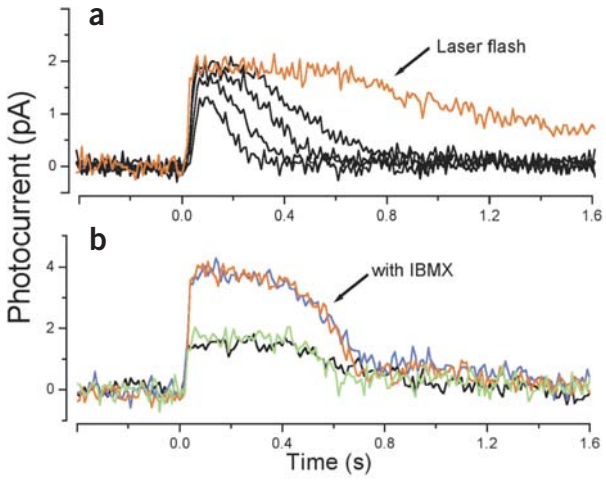


**Figure 3** Rods from *Rpe65*$^{-/-}$ mice show light saturation behavior and have functional cGMP channels. (**a**) Mean responses of four *Rpe65*$^{-/-}$ rods (not part of sample in **Figure 2**) exposed individually to 20-ms flashes at light intensities from near threshold to above apparent saturation (black traces) with 30-s recovery periods after each flash. After an additional 60-s recovery period, a 20-ms flash from the argon laser (red trace) delivered $5.1 \times 10^8$ photons $\mu m^{-2}$ (488 nm) to the same photoreceptor cell. The amplitude of the response did not increase, although response time was prolonged, indicating all cGMP channels were closed at this light intensity. (**b**) Mean responses of four rods to 20-ms flashes of saturating light ($3.4 \times 10^6$ photons $\mu m^{-2}$) in control solution (black trace) and then after perfusion with 100 μM IBMX. Within 1 min, the apparent saturating response doubled in amplitude (blue trace) and stabilized at this value (red trace). Washout of IBMX (green trace) brought the maximum current amplitude back to the preincubation value.

untreated *Rpe65*$^{-/-}$ mice ($P < 0.001$), as reported previously[8,10,11]. These values, however, were less than the mean circulating current and sensitivity recorded from control mice, perhaps reflecting incomplete photopigment regeneration or reduced opsin content arising from shortened outer segments.

### $Na^+/Ca^{2+}$-$K^+$ exchanger mRNA levels are unaltered

The small photocurrent amplitude of *Rpe65*$^{-/-}$ rods might also be caused by compensatory changes in the expression of other phototransduction proteins, such as the sodium, calcium-potassium ($Na^+/Ca^{2+}$-$K^+$) exchanger. To test this, we measured $Na^+/Ca^{2+}$-$K^+$ exchanger mRNA levels by RNase protection assays. We detected no difference in $Na^+/Ca^{2+}$-$K^+$ exchanger mRNA levels in wild-type and *Rpe65*$^{-/-}$ mice (data not shown), suggesting that exchanger expression was unaffected. We did not check protein levels, as antibodies recognizing mouse rod exchanger protein are not currently available.

### Light response waveform is accelerated

Our results thus far (**Figs. 2** and **3**) are consistent with the hypothesis that the relatively large concentration of opsin in *Rpe65*$^{-/-}$ mice activates the phototransduction cascade, producing a decrease in response amplitude much as in a rod whose pigment had been exposed to bleaching light[13,23]. As a further effect of cascade activation, we would expect turn-off of the photoresponse to be accelerated, much as in photoreceptors light-adapted by background light or by pigment bleaching[24]. We compared turn-off of the photoresponse in *Rpe65*$^{-/-}$ and wild-type mice (**Fig. 4**). The smallest response that could be accurately measured from an *Rpe65*$^{-/-}$ rod, representing about 15% of response saturation, is shown as a global average of 1,200 responses from 20 rods, each stimulated with 60 20-ms flashes of 500-nm light at approximately $3.2 \times 10^4$ photons $\mu m^{-2}$. We compare this to the averaged response of 16 wild-type rods to flashes whose intensity (1.2 photons $\mu m^{-2}$) was adjusted to produce a response that was also approximately 15% of saturation (**Fig. 4a**). Shown for comparison is the wild-type single-quantum response, which measures the lower limit of the photoresponse to a single photon of light, averaged from 48 control rods and calculated from the squared mean and variance (for example, ref. 25).

We then normalized these responses (**Fig. 4a**) to their peak amplitudes (**Fig. 4b**). The wild-type control 15% and single-photon traces nearly superimposed, which we expected because both were recorded at light intensities within the linear range of the rod response. The kinetics of response turn-off of *Rpe65*$^{-/-}$ rods, however, were more rapid. We similarly compared brighter flash intensities producing responses at ~35% of saturation in *Rpe65*$^{-/-}$ and wild-type rods (**Fig. 4c**). Again, the normalized mutant rod responses (**Fig. 4d**) declined more rapidly, as predicted.

### Disruption of transducin signaling prevents degeneration

To test whether spontaneous opsin activity caused physiologically relevant degeneration through transducin-mediated signaling, we

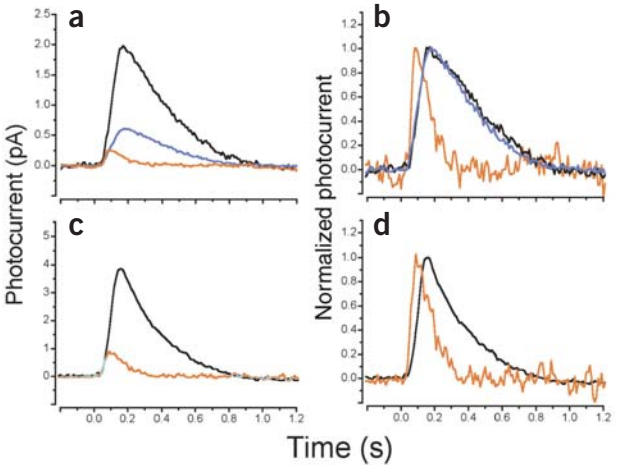


**Figure 4** *Rpe65*$^{-/-}$ rods have accelerated response kinetics. (**a**) Response waveforms of wild-type and *Rpe65*$^{-/-}$ rods near response threshold. The red trace is a global average from 20 *Rpe65*$^{-/-}$ rods to a light intensity that produced a response approximately 15% of saturation. For each rod, the responses to 60 light flashes were averaged (total of 1,200 responses). The black trace shows the averaged response of 16 wild-type rods to flashes whose intensity was adjusted to produce a response that was also approximately 15% of saturation. The blue trace is the single-photon response averaged from 48 wild-type rods. (**b**) Responses shown in **a** normalized to the same peak amplitude. *Rpe65*$^{-/-}$ rods (red trace) showed an accelerated turn-off of the response compared to wild-type rods (black trace) and the single-photon response (blue trace). (**c**) Similar data as in **a** but using brighter flash intensities producing responses at about 35% of saturation. (**d**) Responses shown in **c** normalized to the same peak amplitude.

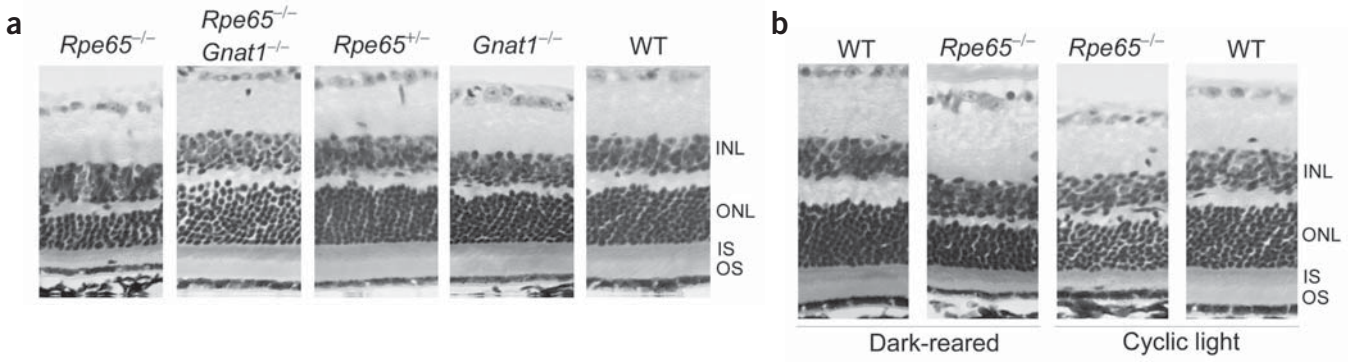


**Figure 5** Abrogation of transducin signaling protects *Rpe65*$^{-/-}$ mice from retinal degeneration, but dark-rearing does not. (**a**) Light micrographs of *Rpe65*$^{-/-}$, *Rpe65*$^{-/-}$ *Gnat1*$^{-/-}$ double mutants, *Rpe65*$^{+/-}$, *Gnat1*$^{-/-}$ and wild-type (WT) mice at 40 weeks of age. Retinal layers are abbreviated as follows: INL, inner nuclear layer; ONL, outer nuclear layer; IS, inner segments; OS, outer segments. ONL cell thickness in retinas of *Rpe65*$^{-/-}$ *Gnat1*$^{-/-}$ double knockout mice was comparable to that in retinas of wild-type mice. Absence of transducin signaling rescued both ONL cell thickness and length of inner segments and outer segments. (**b**) Light micrographs of retinas from 28-week-old *Rpe65*$^{-/-}$ and control mice born and reared in complete darkness compared with retinas of mice reared in cyclic light. Degeneration in dark-reared *Rpe65*$^{-/-}$ retinas as assessed by ONL cell thickness was comparable to that observed in *Rpe65*$^{-/-}$ mice reared in cyclic light. No degeneration was observed in wild-type (WT) mice reared in complete darkness or in cyclic light.

examined retinal morphology of *Rpe65*$^{-/-}$ mice on a transducin-null (*Gnat1*$^{-/-}$) genetic background (**Fig. 5**). If transducin-mediated opsin signaling caused degeneration, we predicted that *Rpe65*$^{-/-}$ *Gnat1*$^{-/-}$ mice would be protected from degeneration relative to *Rpe65*$^{-/-}$ *Gnat1*$^{+/+}$ mice. The transducin-null mutation alone does not cause degeneration[26] (**Fig. 5a**).

We examined retinal morphology in mice at 15, 28 (**Supplementary Fig. 1** online) and 40 weeks (**Fig. 5a**) of age. We assessed the severity of retinal degeneration by counting the rows of surviving photoreceptor nuclei in the outer nuclear layer (ONL). At 15 weeks of age, the ONL in retinas of *Rpe65*$^{-/-}$ mice was 1–2 rows thinner and the outer segment to inner segment ratio (OS:IS) was slightly smaller than in age-matched wild-type mice (**Supplementary Figs. 1** and **2** and **Supplementary Table 1** online). At 28 weeks of age, the ONL in *Rpe65*$^{-/-}$ mice retained 7–8 rows as compared to 10 rows in wild-type mice, and there was a clear decrease in the OS:IS ratio in mutant (1:1) relative to wild-type mice (1.5:1). At 40 weeks of age, *Rpe65*$^{-/-}$ mice retained 6–7 rows of photoreceptor cells, nearly half that observed in retinas of age-matched wild-type mice. Photoreceptor outer and inner segments were considerably shortened. Age-matched wild-type mice retained 9–11 rows of nuclei (**Fig. 5a** and **Supplementary Fig. 2** and **Supplementary Table 1** online). Neither retinas from age-matched heterozygous *Rpe65* (*Rpe65*$^{+/-}$) mice nor those of *Gnat1*$^{-/-}$ mice showed evidence of degeneration; their retinal morphology was comparable to that of wild-type mice (**Fig. 5a**).

*Rpe65*$^{-/-}$ mice on a *Gnat1*$^{-/-}$ background were markedly and completely protected from degeneration (**Fig. 5a** and **Supplementary Fig. 2** and **Supplementary Table 1** online). ONL thicknesses in 40-week-old *Rpe65*$^{-/-}$ *Gnat1*$^{-/-}$ double mutant mice were restored to 9–10 rows, comparable to age-matched wild-type control mice and greater than the 6–7 rows retained in age-matched *Rpe65*$^{-/-}$ retinas. The OS:IS ratio in *Rpe65*$^{-/-}$ *Gnat1*$^{-/-}$ mice was also restored (**Fig. 5a**). Thus, the absence of functional transducin blocked degeneration in *Rpe65*$^{-/-}$ mice.

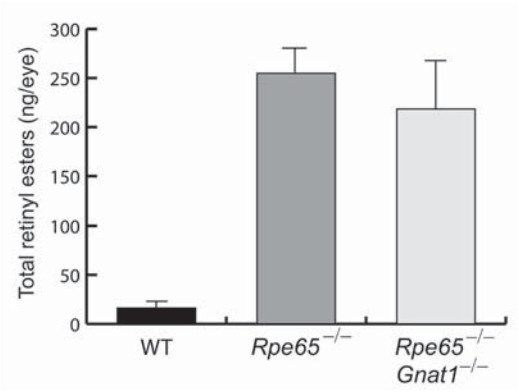


**Figure 6** Retinyl ester levels in wild-type (WT), *Rpe65*$^{-/-}$ and *Rpe65*$^{-/-}$ *Gnat1*$^{-/-}$ mice. Total retinyl esters from 6-month-old mice were compared. The values are indicated as means ± s.d. per eye for 3–5 mice of each genotype. Retinyl ester levels in the degenerating *Rpe65*$^{-/-}$ mice were comparable to those in the non-degenerating *Rpe65*$^{-/-}$ *Gnat1*$^{-/-}$ mice. Both were elevated relative to levels in wild-type mice. There was no statistical difference between *Rpe65*$^{-/-}$ and *Rpe65*$^{-/-}$ *Gnat1*$^{-/-}$ double mutants.

### Dark-rearing does not prevent degeneration in *Rpe65*$^{-/-}$ mice

If spontaneous, light-independent opsin activity were the cause of degeneration in *Rpe65*$^{-/-}$ mice, we would predict that dark-rearing would not be protective. *Rpe65*$^{-/-}$ mice were born and raised in darkness to 28 and 40 weeks of age. Dark-reared *Rpe65*$^{-/-}$ mice were not protected from degeneration (**Fig. 5b**). Age-matched, dark-reared, wild-type control mice showed no degeneration. These results indicate that degeneration in *Rpe65*$^{-/-}$ mice occurs in a light-independent fashion, consistent with signal transduction by spontaneous opsin activity.

### Retinyl ester levels are high in *Rpe65*$^{-/-}$ *Gnat1*$^{-/-}$ mice

We further asked whether retinyl esters continued to accumulate in *Rpe65*$^{-/-}$ *Gnat1*$^{-/-}$ knockout mice. We measured retinyl ester levels in eyecups collected from six-month-old wild-type, *Rpe65*$^{-/-}$ and *Rpe65*$^{-/-}$ *Gnat1*$^{-/-}$ mice (**Fig. 6**). Consistent with previous reports[6,10,11], retinyl ester levels in *Rpe65*$^{-/-}$ mice (mean ± s.d. 254.8 ± 22 ng per eye; $n = 3$) were 16 times higher than in control mice (16.2 ± 5 ng per eye; $n = 3$). Retinyl ester levels in non-degenerating *Rpe65*$^{-/-}$ *Gnat1*$^{-/-}$ retinas remained elevated (218.4 ± 50 ng per eye; $n = 5$), conclusively showing that retinyl ester accumulation does not cause degeneration.

### $Ca^{2+}$ concentration is low in *Rpe65*$^{-/-}$ photoreceptors

A hallmark feature of visual signaling is low intracellular calcium levels resulting from signal-mediated closure of the cGMP-gated channels coupled with calcium extrusion by the $Na^+/Ca^{2+}$-$K^+$ exchanger.

If opsin in *Rpe65*$^{-/-}$ mice activated transduction in darkness, we would expect *Rpe65*$^{-/-}$ rods to have a lower than normal free $Ca^{2+}$ concentration (**Fig. 1b**), as these rods should behave like normal rods exposed to bright bleaching light[27]. The $Ca^{2+}$ concentration in *Rpe65*$^{-/-}$ *Gnat1*$^{-/-}$ rods, however, would be predicted to be normal.

To test these predictions, we compared the free $Ca^{2+}$ concentration in *Rpe65*$^{-/-}$ and *Rpe65*$^{-/-}$ *Gnat1*$^{-/-}$ rod outer segments (**Fig. 7**) using laser-spot fluorescence microscopy and the $Ca^{2+}$ dye fluo-5F[28]. After exposure to laser light, fluorescence of rods from *Rpe65*$^{-/-}$ mice decreased rapidly, reflecting a light-induced decrease in $Ca^{2+}$ concentration. In comparison, baseline (dark) fluorescence was greater from wild-type or *Rpe65*$^{-/-}$ *Gnat1*$^{-/-}$ rods, and, as expected, there was no light-dependent decrease in fluorescence in *Rpe65*$^{-/-}$ *Gnat1*$^{-/-}$ rods[28]. The lower baseline fluorescence in rods from dark-adapted *Rpe65*$^{-/-}$ retinas and the greater fluorescence in the *Rpe65*$^{-/-}$ *Gnat1*$^{-/-}$ double knockout mice reflects spontaneous, opsin-mediated closure of the cGMP-gated channels in *Rpe65*$^{-/-}$ mice.

Estimates of absolute free $Ca^{2+}$ concentration in darkness or light (**Table 1**) obtained as previously described[28] reinforced this conclusion. *Rpe65*$^{-/-}$ rods had less free $Ca^{2+}$ in darkness than either normal or *Rpe65*$^{-/-}$ *Gnat1*$^{-/-}$ rods. There was no statistically significant difference in the $Ca^{2+}$ concentration in darkness between control and *Rpe65*$^{-/-}$ *Gnat1*$^{-/-}$ rods or after exposure to bright light between control and *Rpe65*$^{-/-}$ rods. Thus, not only do rods of dark-adapted *Rpe65*$^{-/-}$ mice have less intracellular calcium, but blocking transducin signaling also restores intracellular calcium in *Rpe65*$^{-/-}$ *Gnat1*$^{-/-}$ mice to concentrations comparable to those observed in dark-adapted wild-type mice.

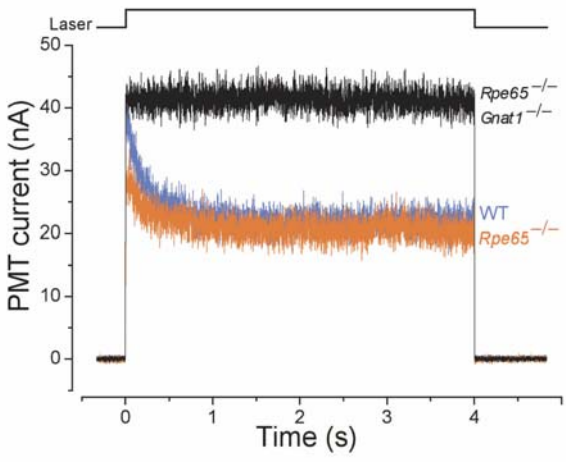


**Figure 7** Free $Ca^{2+}$ concentration in rods from wild-type (WT; blue), *Rpe65*$^{-/-}$ (red) and *Rpe65*$^{-/-}$ *Gnat1*$^{-/-}$ (black) mice. Rods were loaded with the $Ca^{2+}$-sensitive dye fluo-5F and exposed to a 4-s laser light at $1.8 \times 10^{10}$ photons $\mu m^{-2}$ $s^{-1}$. Fluorescence emission was measured as a photomultiplier tube (PMT) current. The wild-type, *Rpe65*$^{-/-}$ and *Rpe65*$^{-/-}$ *Gnat1*$^{-/-}$ traces are the mean of 8, 7 and 12 determinations, respectively. We fit the individual decreases in fluorescence in the *Rpe65*$^{-/-}$ rods with the double exponential decay function used to analyze wild-type rods[28]. The faster of the two time constants for *Rpe65*$^{-/-}$ rods ($\tau_1 = 169 \pm 28$ ms; $n = 7$) was not significantly different from that for wild-type mice ($\tau_1 = 148 \pm 30$ ms; $n = 8$). Wild-type and *Rpe65*$^{-/-}$ *Gnat1*$^{-/-}$ rods showed a higher initial value of fluorescence than *Rpe65*$^{-/-}$ rods, reflecting the relatively higher dark-adapted $Ca^{2+}$ concentration (see **Table 1**).

## DISCUSSION

These experiments show that rods of *Rpe65*$^{-/-}$ mice behave as if strongly adapted by background light or previous light bleaching, even when they were not exposed to light or bleaching. The rods have low circulating current (**Figs. 2** and **3**), low light sensitivity (**Fig. 2**) and accelerated kinetics of response decay (**Fig. 4**). *Rpe65*$^{-/-}$ rods contain a high concentration of the apoprotein opsin, mostly unphosphorylated and unbound to arrestin[6,8,9]. Because opsin activates the visual cascade at a low level[13–15], we conclude that spontaneous opsin activity in *Rpe65*$^{-/-}$ mice activates PDE, leading to closure of cGMP-gated channels. The low circulating current and small intracellular $Ca^{2+}$ concentration of dark-adapted *Rpe65*$^{-/-}$ rods (**Fig. 7** and **Table 1**) must result from opsin activation of the cascade.

Deleting *Gnat1* eliminated degeneration in *Rpe65*$^{-/-}$ mice (**Fig. 5a**), although dark-rearing had no effect (**Fig. 5b**), confirming that light-independent opsin activation caused cell death. *Rpe65*$^{-/-}$ *Gnat1*$^{-/-}$ double knockout mice had normal retinal morphology (**Fig. 5a**) despite accumulating retinyl esters to high levels (**Fig. 6**), indicating that ester accumulation does not contribute to degeneration.

How activation of the cascade by opsin apoprotein causes degeneration is unknown. A high concentration of opsin apoprotein might produce structural weakness in the outer segment disk membrane[6], but this seems an unlikely mechanism for degeneration. Total opsin levels in *Rpe65*$^{-/-}$ retinas are lower than rhodopsin levels in wild-type mouse retinas (refs. 6,9 and data not shown). Total opsin levels in *Rpe65*$^{-/-}$ *Gnat1*$^{-/-}$ double knockout mice, however, are similar to levels in age-matched, wild-type mice (data not shown) at 28 and 40 weeks of age, when decreased opsin levels and degeneration in *Rpe65*$^{-/-}$ mice are evident. Thus, total opsin levels in nondegenerating *Rpe65*$^{-/-}$ *Gnat1*$^{-/-}$ retinas are higher than in age-matched, degenerating *Rpe65*$^{-/-}$ retinas.

Alternatively, the low $Ca^{2+}$ concentration in *Rpe65*$^{-/-}$ rod outer segments might trigger apoptosis, as previously suggested for developing neurons (for example, ref. 29) and photoreceptors[17]. *Rpe65*$^{-/-}$ rods have a low concentration of free $Ca^{2+}$ in the outer segment (**Fig. 7** and **Table 1**), but the concentration of $Ca^{2+}$ in rods from non-degenerating *Rpe65*$^{-/-}$ *Gnat1*$^{-/-}$ double mutant mice is nearly normal.

One difficulty with this hypothesis is that the $Ca^{2+}$ concentration in *Rpe65*$^{-/-}$ mice is about half that observed in wild-type mice (**Table 1**), even though circulating current is 10–15% of normal. As free $Ca^{2+}$ concentration and current are linearly related[30,31], one would expect $Ca^{2+}$ to be even lower in *Rpe65*$^{-/-}$ mice. We found no evidence for altered cGMP-gated channel function or rod exchanger mRNA levels that might account for this difference. The discrepancy may reflect changes in the morphological or physiological state of *Rpe65*$^{-/-}$ rods; when *Rpe65*$^{-/-}$ rods were given 11-*cis*-retinal to regenerate rhodopsin, the free $Ca^{2+}$ concentration rose to the abnormally high value of ~600 nM, twice that observed in dark-adapted wild-type mice (M.L.W. and G.L.F., unpublished observations). More experiments are needed to determine whether lowered $Ca^{2+}$ concentration has a role in cell death during constitutive activation.

Degeneration in *Rpe65*$^{-/-}$ mice may also be influenced by aberrant transducin localization in rods. In light-exposed wild-type mice, transducin rapidly translocates from rod outer to inner segments[32].

**Table 1 Calcium concentrations**

| | *n*[a] | Dark[b] (nM) | Saturating light[b,c] (nM) |
|---|---|---|---|
| Control (wild-type) | 6 | 246 ± 37 | 60 ± 10 |
| *Rpe65*$^{-/-}$ | 7 | 138 ± 14 | 40 ± 5 |
| *Rpe65*$^{-/-}$ *Gnat1*$^{-/-}$ | 12 | 307 ± 37 | |

[a]Number of determinations. [b]Mean ± s.e.m. [c]Saturating illumination is from the laser exposure used to measure the dye fluorescence.

But transducin translocation is defective in *Rpe65*$^{-/-}$ mice[33]; light does not induce transducin migration to the inner segment. The inappropriate colocalization of unliganded opsin and rod transducin in *Rpe65*$^{-/-}$ rod outer segments may affect the level of constant transducin signaling and, therefore, the rate of retinal degeneration[17]. One important role for the rapid, light-induced translocation of transducin to the inner segment may be to reduce signaling during continuous light exposure.

The accelerated response kinetics of *Rpe65*$^{-/-}$ rods (**Fig. 4**) were not observed in a previous study[11]. This difference probably results from intrinsic variability in rod response waveform and the much larger sample number in the present experiments (see legend to **Fig. 4**). It is notable that rods partially regenerated with 9-*cis*-retinal have accelerated kinetics of response decay, which has previously been attributed to opsin activation of the cascade[11], consistent with our conclusions.

In conclusion, these studies show that constitutive opsin signaling causes retinal degeneration in rod cells of the *Rpe65*$^{-/-}$ mouse. The contribution of all-*trans*-retinyl ester accumulation is minimal. As *Rpe65*$^{-/-}$ mice are also a model of prolonged vitamin A deprivation, our experiments may also confirm an explanation[16] as to why rods deprived of retinal, but containing opsin, show progressive degeneration[34,35]. For the first time, we show that activation of an unliganded G-protein-coupled receptor molecule lacking mutations in its sequence[8] causes disease from abnormal signaling activity in established models of human disease. It will be interesting to determine whether other G-protein-coupled receptor molecules similarly contribute to human disease.

## METHODS

**Mice.** We handled mice in accordance with the guidelines provided by the Association for Research in Vision and Ophthalmology and the Tufts University Institutional Animal Care and Use Committee. *Rpe65*$^{-/-}$ (ref. 6) and *Gnat1*$^{-/-}$ (ref. 26) mice have been previously described. We housed mice in standard filter-top cages and maintained them either on a 14 h light:10 h dark or a 12 h light:12 h dark cycle. *Gnat1*$^{-/-}$ and *Rpe65*$^{-/-}$ double knockout mice were generated by crossbreeding *Rpe65*$^{-/-}$ mice with *Gnat1*$^{-/-}$ mice. Dark-reared mice were raised in a ventilated dark chamber (Plastic Designs).

**Genotype analysis.** We carried out PCR on genomic DNA prepared from tail biopsy samples to screen for the presence of *Rpe65* or *Gnat1* as follows: denaturation at 95 °C for 4 min, followed by 27 cycles of 95 °C for 1 min, 61 °C for 1 min and 72 °C for 1 min. We used triple primer sets to amplify and distinguish either the *Rpe65*- or the *Gnat1*-null genes from the wild-type gene. Primers for *Rpe65*$^{-/-}$ transgenic mice were as previously described[6]. Primer sets for transducin gene amplification will be provided on request.

**Chemicals and solutions.** R. Crouch (Medical University of South Carolina) provided 11-*cis*-retinal. We purchased the fluorescent $Ca^{2+}$ dye fluo-5F as the acetoxymethyl ester from Molecular Probes. We purchased all other chemicals from Sigma Chemical. We carried out dissections and incubations with acetoxymethyl ester dye and 11-*cis*-retinal in Locke's solution (140 mM NaCl, 3.6 mM KCl, 2.4 mM $MgCl_2$, 1.2 mM $CaCl_2$, 20 μM EDTA, 3.0 mM HEPES buffer, 10 mM glucose and 5 mM sodium ascorbate, pH 7.4). During suction pipette and fluorescence measurements, we continuously perfused photoreceptors with Dulbecco's modified Eagle medium (Sigma Chemical, D-2902), supplemented with 15 mM $NaHCO_3$, 2 mM sodium succinate, 0.5 mM sodium glutamate, 2 mM sodium gluconate and 5 mM NaCl, bubbled with 5% $CO_2$. The pH was adjusted to 7.4 and the temperature was 33–37 °C. We filled the suction pipette and bath ground electrode with Locke's solution without glucose or ascorbate. We assessed the purity and concentration of the 11-*cis*-retinal chromophore by spectrophotometry before each experiment.

**Dissection, dye-loading and 11-*cis*-retinal incubation.** We placed mice 3–10 weeks old (maintained on a 12 h light:12 h dark cycle) in total darkness for 3 h before the experiments. Under dim red light, we killed mice by cervical dislocation, excised the eyes, trimmed off fat and extraocular muscle and washed them with 1–2 ml cold Locke's solution. Under infrared illumination, we carried out the rest of the dissection with an infrared-sensitive television camera (charge-coupled device camera model OS-40D, Mintron USA) or an infrared-sensitive viewer (FJW Optical Systems). We hemisected the eye with a razor blade and discarded the front of the eye (with lens). We cut the eyecup, retina-side up, into two roughly equal pieces by slicing close to the optic nerve head. We reserved three pieces of eyecup on ice in total darkness in Locke's solution. We placed the remaining piece in Locke's solution into a 35-mm petri dish whose bottom had been coated with Sylgard (Dow Corning). We carefully peeled the retina from the pigment epithelium/eyecup, inverted it (receptor-side up) onto the Sylgard surface and finely chopped it with a shard of razor blade held by a hemostat. We pipetted the retinal pieces into Locke's solution on the stage of an inverted microscope for electrical recording. For fluorescence measurements of $Ca^{2+}$, we incubated retinal pieces for 30 min in Locke's solution containing 10 μM fluo-5F-acetoxymethyl ester. To regenerate the photopigment, we exposed rods for 30 min to Ringer's solution containing 30 μM 11-*cis*-retinal from an ethanolic stock solution.

**Recording of light responses.** We recorded suction-pipette currents by conventional methods. Responses were low-pass filtered at 35 Hz and digitized at a sampling rate of 100 Hz (PCLAMP, Axon Instruments) with a PC-compatible computer. We delivered light stimuli from a dual-beam optical bench through a 500-nm interference filter, controlled stimulus intensity with absorptive neutral density filters and measured intensity with a calibrated silicon photodiode (Graseby Optronics). In some experiments, we stimulated rods with white light, whose effective intensity was estimated by comparing the relative sensitivity of the electrical response of control mice to dim flashes of white and 500-nm light. We estimated rhodopsin bleaching from the photosensitivity for a vitamin-$A_2$-based pigment in solution[36], corrected for the difference in dichroism in free solution and in disk membranes[37]. In a few experiments, we stimulated rods with light from the laser (488 nm), which we calibrated in the same way as light from the optical bench. We allowed rods exposed to multiple flashes to recover for 30 s or 60 s after each flash. We determined the single-photon response by squaring the mean response of 30–60 flashes to the same dim intensity and comparing the squared mean to the waveform of the time-dependent variance by bringing the two into alignment at their rising phases. This provides an estimate of $1/n$, where $n$ is the mean number of rhodopsins activated by the dim flash. We divided the mean response to the flash by $n$ to give the single-photon response.

**Retinal morphology.** We oriented right eyes by a cautery mark to the superior pole of the eye before enucleation. We punctured the anterior eye segment with a needle and immediately immersed the eye in a fixative of 4% paraformaldehyde/0.1% glutaraldehyde in 0.1 M phosphate buffer (pH 7.4) at 4 °C overnight. The eye was then dehydrated in a graded series of alcohol and embedded in paraffin. We bisected eyes along the vertical meridian through the optic nerve head and stained with hematoxylin and eosin for light microscopy. We carried out morphological analysis by counting rows of photoreceptor cells in the ONL from four different areas in the central and mid-peripheral retina across both the superior and inferior hemispheres. We averaged the resulting numbers for each retina. We took the counts from five or more representative mice for each genotype at each time point. We used the two-tailed Student's *t*-test to compare paired data from age-matched wild-type and mutant mice.

**HPLC analysis of retinyl ester content.** We dark-adapted overnight six-month-old wild-type, *Rpe65*$^{-/-}$ and *Rpe65*$^{-/-}$ *Gnat1*$^{-/-}$ double mutant mice. We dissected out the anterior segments, lens and retinas under infrared illumination. We homogenized eye cups from a single mouse in 200 μl phosphate-buffered saline and extracted retinyl esters with methanol/hexane. We assessed levels of retinyl esters by reverse-phase HPLC analysis[38–41]. We equipped the HPLC system with a Pecosphere-3 C18 column (Perkin-Elmer) and a Waters 996 Photodiode Array Detector with the wavelength set at 325 nm for retinol and retinyl esters and 380 nm for retinal.

**Determination of free $Ca^{2+}$ concentration.** Methods for measuring calcium in rod outer segments have been described previously[27,28,42]. We excited fluorescence (wavelength, 488 nm) with an argon laser (American Laser Corporation) and collected fluorescence with a 505-nm dichroic and a 510-nm long-pass filter (Omega Optical). We recorded fluorescence from the outer segments of single mouse rods either fully isolated or protruding from small chunks of retina. We placed a miniature thermocouple (diameter 0.05 mm, T-type, Cu-CuNi; Omega Engineering) within 0.5 mm of the rod and monitored the temperature with a digital thermometer at 0.1 °C resolution (Model HH-25TC, Omega Engineering). We noted the temperature at the time of each fluorescence measurement and used it to correct the dissociation constant of $Ca^{2+}$ binding to the dye as described[28].

To prevent dye bleaching, we reduced the unattenuated intensity of the laser to 2–5 × $10^{10}$ photons $\mu m^{-2}$ $s^{-1}$ with reflective neutral density filters (Newport). We measured fluorescence with a low-dark-count photomultiplier tube with a restricted photocathode (Model 9130/100A, Electron Tubes) and amplified the current with a low-noise, current-to-voltage converter (PDA-700, Terahertz Technology), low-pass filtered with an 8-pole Bessel filter (Frequency Devices) and digitized with a PC-compatible computer. The data were filtered at 1 kHz and acquired at 2 kHz.

We estimated the intracellular concentration of $Ca^{2+}$ in darkness and after illumination, from the initial and steady-state fluorescence after exposure to the bright light of the laser. We used the Michaelis-Menten equation together with estimates of the minimum and maximum fluorescence ($F_{min}$ and $F_{max}$) and the dissociation constant ($K_d$) to convert fluorescence into $[Ca^{2+}]_i$ (refs. 27,28,42,43). We estimated the $F_{min}$ by exposing the rod to a zero-$Ca^{2+}$/ionomycin solution (140 mM NaCl, 3.6 mM KCl, 3.08 mM $MgCl_2$, 2.0 mM EGTA, 3.0 mM HEPES buffer with 10 µM ionomycin, pH 7.4). When the fluorescence reached a steady minimum value, we exposed the rod to a high-$Ca^{2+}$/ionomycin solution (50 mM $CaCl_2$, 3.6 mM KCl, 3.0 mM HEPES buffer, 140 mM sucrose with 10 µM ionomycin, pH 7.4) to estimate $F_{max}$. The $K_d$ varied from 400 nM to 543 nM[28] over the temperature range used in these determinations (33–37 °C).

*Note: Supplementary information is available on the Nature Genetics website.*

ACKNOWLEDGMENTS

We thank M. Cilluffo for help with animal care, M. Fain for drawing Fig. 1, F. Celestin for assistance with histological sections, M. C. Cornwall and H. R. Matthews for assistance with early experiments and M. S. Obin for discussion and comments. Support for this research was provided by the US National Institutes of Health (to G.L.F., J.L. and Z.W.; Core Grants for Vision Research to the Jules Stein Eye Institute and Tufts Center for Vision Research) and the Massachusetts Lions Eye Research Fund (an institutional grant to the Department of Ophthalmology, New England Medical Center).

COMPETING INTERESTS STATEMENT

The authors declare that they have no competing financial interests.

Received 25 June; accepted 26 August 2003
Published online at http://www.nature.com/naturegenetics/

1. Morimura, H. *et al.* Mutations in the *RPE65* gene in patients with autosomal recessive retinitis pigmentosa or Leber congenital amaurosis. *Proc. Natl. Acad. Sci. USA* **95**, 3088–3093 (1998).
2. Gu, S.M. *et al.* Mutations in *RPE65* cause autosomal recessive childhood-onset severe retinal dystrophy. *Nat. Genet.* **17**, 194–197 (1997).
3. Marlhens, F. *et al.* Mutations in *RPE65* cause Leber's congenital amaurosis. *Nat. Genet.* **17**, 139–141 (1997).
4. Felius, J. *et al.* Clinical course and visual function in a family with mutations in the *RPE65* gene. *Arch. Ophthalmol.* **120**, 55–61 (2002).
5. Lorenz, B. *et al.* Early-onset severe rod-cone dystrophy in young children with *RPE65* mutations. *Invest. Ophthalmol. Vis. Sci.* **41**, 2735–2742 (2000).
6. Redmond, T.M. *et al.* Rpe65 is necessary for production of 11-*cis*-vitamin A in the retinal visual cycle. *Nat. Genet.* **20**, 344–351 (1998).
7. Seeliger, M.W. *et al.* New views on RPE65 deficiency: the rod system is the source of vision in a mouse model of Leber congenital amaurosis. *Nat. Genet.* **29**, 70–74 (2001).
8. Ablonczy, Z. *et al.* 11-*cis*-retinal reduces constitutive opsin phosphorylation and improves quantum catch in retinoid-deficient mouse rod photoreceptors. *J. Biol. Chem.* **277**, 40491–40498 (2002).
9. Rohrer, B. *et al.* Correlation of regenerable opsin with rod ERG signal in *Rpe65*$^{-/-}$ mice during development and aging. *Invest. Ophthalmol. Vis. Sci.* **44**, 310–315 (2003).
10. Van Hooser, J.P. *et al.* Rapid restoration of visual pigment and function with oral retinoid in a mouse model of childhood blindness. *Proc. Natl. Acad. Sci. USA* **97**, 8623–8628 (2000).
11. Van Hooser, J.P. *et al.* Recovery of visual functions in a mouse model of Leber congenital amaurosis. *J. Biol. Chem.* **277**, 19173–19182 (2002).
12. Surya, A. & Knox, B. Modulation of opsin apoprotein activity by retinal. Dark activity of rhodopsin formed at low temperature. *J. Biol. Chem.* **272**, 21745–21750 (1997).
13. Cornwall, M.C. & Fain, G.L. Bleached pigment activates transduction in isolated rods of the salamander retina. *J. Physiol.* **480**, 261–279 (1994).
14. Cornwall, M.C., Matthews, H.R., Crouch, R.K. & Fain, G.L. Bleached pigment activates transduction in salamander cones. *J. Gen. Physiol.* **106**, 543–557 (1995).
15. Melia, T.J., Jr., Cowan, C.W., Angleson, J.K. & Wensel, T.G. A comparison of the efficiency of G protein activation by ligand-free and light-activated forms of rhodopsin. *Biophys. J.* **73**, 3182–3191 (1997).
16. Fain, G.L. & Lisman, J.E. Photoreceptor degeneration in vitamin A deprivation and retinitis pigmentosa: the equivalent light hypothesis. *Exp. Eye Res.* **57**, 335–340 (1993).
17. Fain, G.L. & Lisman, J.E. Light, $Ca^{2+}$, and photoreceptor death: new evidence for the equivalent-light hypothesis from arrestin knockout mice. *Invest. Ophthalmol. Vis. Sci.* **40**, 2770–2772 (1999).
18. Jin, S., Cornwall, M.C. & Oprian, D.D. Opsin activation as a cause of congenital night blindness. *Nat. Neurosci.* **6**, 731–735 (2003).
19. Hao, W. *et al.* Evidence for two apoptotic pathways in light-induced retinal degeneration. *Nat. Genet.* **32**, 254–260 (2002).
20. Baylor, D.A., Lamb, T.D. & Yau, K.W. The membrane current of single rod outer segments. *J. Physiol.* **288**, 589–611 (1979).
21. Beavo, J.A. *et al.* Effects of xanthine derivatives on lipolysis and on adenosine 3′,5′-monophosphate phosphodiesterase activity. *Mol. Pharmacol.* **6**, 597–603 (1970).
22. Cervetto, L. & McNaughton, P.A. The effects of phosphodiesterase inhibitors and lanthanum ions on the light-sensitive current of toad retinal rods. *J. Physiol.* **370**, 91–109 (1986).
23. Cornwall, M.C., Fein, A. & MacNichol, E.F., Jr. Cellular mechanisms that underlie bleaching and background adaptation. *J. Gen. Physiol.* **96**, 345–372 (1990).
24. Fain, G.L., Matthews, H.R., Cornwall, M.C. & Koutalos, Y. Adaptation in vertebrate photoreceptors. *Physiol. Rev.* **81**, 117–151 (2001).
25. Chen, C.K. *et al.* Slowed recovery of rod photoresponse in mice lacking the GTPase accelerating protein RGS9-1. *Nature* **403**, 557–560 (2000).
26. Calvert, P.D. *et al.* Phototransduction in transgenic mice after targeted deletion of the rod transducin α-subunit. *Proc. Natl. Acad. Sci. USA* **97**, 13913–13918 (2000).
27. Sampath, A.P., Matthews, H.R., Cornwall, M.C. & Fain, G.L. Bleached pigment produces a maintained decrease in outer segment $Ca^{2+}$ in salamander rods. *J. Gen. Physiol.* **111**, 53–64 (1998).
28. Woodruff, M.L. *et al.* Measurement of cytoplasmic calcium concentration in the rods of wild-type and transducin knock-out mice. *J. Physiol.* **542**, 843–854 (2002).
29. Franklin, J.L., Sanz-Rodriguez, C., Juhasz, A., Deckwerth, T.L. & Johnson, E.M.Jr. Chronic depolarization prevents programmed death of sympathetic neurons *in vitro* but does not support growth: requirement for $Ca^{2+}$ influx but not *Trk* activation. *J. Neurosci.* **15**, 643–664 (1995).
30. Sampath, A.P., Matthews, H.R., Cornwall, M.C., Bandarchi, J. & Fain, G.L. Light-dependent changes in outer segment free-$Ca^{2+}$ concentration in salamander cone photoreceptors. *J. Gen. Physiol.* **113**, 267–277 (1999).
31. Matthews, H.R. & Fain, G.L. The effect of light on outer segment calcium in salamander rods. *J. Physiol.* (in the press).
32. Sokolov, M. *et al.* Massive light-driven translocation of transducin between the two major compartments of rod cells: a novel mechanism of light adaptation. *Neuron* **33**, 95–106 (2002).
33. Mendez, A., Lem, J., Simon, M. & Chen, J. Light-dependent translocation of arrestin in the absence of rhodopsin phosphorylation and transducin signaling. *J. Neurosci.* **23**, 3124–3129 (2003).
34. Dowling, J.E. & Wald, G. Vitamin A deficiency and night blindness. *Proc. Natl. Acad. Sci. USA* **44**, 648–661 (1958).
35. Dowling, J.E. & Wald, G. The biological activity of vitamin A acid. *Proc. Natl. Acad. Sci. USA* **46**, 587–608 (1960).
36. Dartnall, H.J.A. Photosensitivity. in *Handbook of Sensory Physiology* vol. VII/1 (ed. Dartnall, H.J.A.) 122–145 (Springer, Berlin, 1972).
37. Jones, G.J., Fein, A., MacNichol, E.F., Jr. & Cornwall, M.C. Visual pigment bleaching in isolated salamander retinal cones. Microspectrophotometry and light adaptation. *J. Gen. Physiol.* **102**, 483–502 (1993).
38. Tang, G., Dolnikowski, G.G., Blanco, M.C., Fox, J.G. & Russel, R.M. Serum carotenoids and retinoids in ferrets fed canthaxanthin. *J. Nutr. Biochem.* **4**, 58–63 (1993).
39. Garwin, G.G. & Saari, J.C. High-performance liquid chromatography analysis of visual cycle retinoids. *Meth. Enzymol.* **316**, 313–324 (2000).
40. Carter-Dawson, L. *et al.* Rhodopsin, 11-*cis* vitamin A, and interstitial retinol-binding protein (IRBP) during retinal development in normal and *rd* mutant mice. *Dev. Biol.* **116**, 431–438 (1986).
41. Palczewski, K. *et al.* Kinetics of visual pigment regeneration in excised mouse eyes and in mice with a targeted disruption of the gene encoding interphotoreceptor retinol-binding protein or arrestin. *Biochemistry* **38**, 12012–12019 (1999).
42. Matthews, H.R. & Fain, G.L. Time course and magnitude of the calcium release induced by bright light in salamander rods. *J. Physiol.* **542**, 829–841 (2002).
43. Grynkiewicz, G., Poenie, M. & Tsien, R.Y. A new generation of $Ca^{2+}$ indicators with greatly improved fluorescence properties. *J. Biol. Chem.* **260**, 3440–3450 (1985).